Polymer Bulletin (2024) 81:10787–10803
https://doi.org/10.1007/s00289-024-05180-6

ORIGINAL PAPER

Electrospun nanofibers incorporated with β-cyclodextrin as a delivery system of doxorubicin

Mohammad H. Hamzeh[1] · Elham Arkan[2] · Mohammad Jafarzadeh[1] · Rana A. Ghaleb[3] · Hosna Alvandi[2]

Received: 19 July 2023 / Revised: 10 January 2024 / Accepted: 31 January 2024 /
Published online: 17 March 2024

Abstract

In the present study, a drug-delivery system based on electrospun nanofiber was developed. Polyamide (PA) as a fibers matrix was employed for the delivery of the anticancer drug doxorubicin (DOX). The nanofiber (NFs) was initially modified by incorporating β-cyclodextrin (β-CD) to generate an inclusion complex of β-CD and drug. The modified nanofiber was subsequently fabricated via an electrospinning approach of DOX/β-CD-incorporated PA. For understanding the role of β-CD in the inclusion of DOX, a DOX-incorporated nanofiber (i.e., PA/β-CD) was fabricated for comparison. β-CD enhanced the loading of DOX into PA NFs, resulting in an increased loading efficiency of 56% (PA/β-CD/DOX), compared to 47% for PA/DOX. In addition, the release profile of DOX and the effect of β-CD on the release behavior were investigated. The results demonstrated a substantial release of the drug (total release = ~92%) from PA/β-CD/DOX NFs, with a slower release rate (within 4 days) compared to PA/DOX without β-CD (total release = ~77%). Consequently, β-CD played a significant role in the sustained release of the drug. The viability of prostate cancer and LNCap cells in response to the drug was assessed for the NFs. The decreased cell viability observed in PA/β-CD/DOX indicates a sustained and controlled release behavior for this drug carrier system.

✉ Mohammad Jafarzadeh
m.jafar@razi.ac.ir; mjafarzadeh5@gmail.com

[1] Faculty of Chemistry, Razi University, Kermanshah 67149-67346, Iran

[2] Nano Drug Delivery Research Center, Health Technology Institute, Kermanshah University of Medical Sciences, Kermanshah, Iran

[3] College of Medicine, University of Babylon, Babylon, Iraq

Graphical abstract

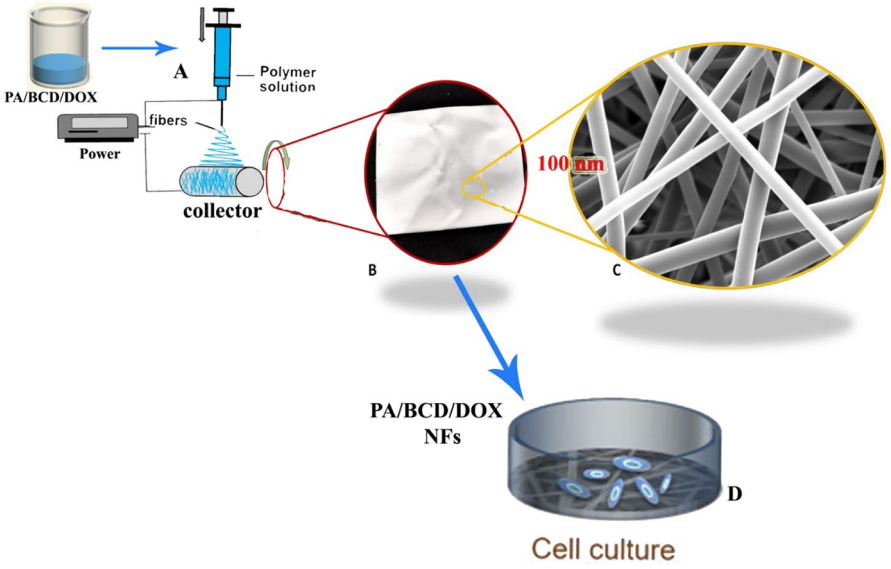

Keywords Electrospun nanofibers · Polyamide · Doxorubicin · β-Cyclodextrins

Introduction

Cancer is one of the diseases with a relatively high rate of mortality for humans. Numerous strategies have been applied to halt cancer cell proliferation and recurrence, such as chemotherapy and radiotherapy after surgery. The challenge is the emergence of adverse effects and poor efficacy, as the anticancer drugs affect both cancer and healthy cells [1]. Therefore, sustained and targeted drug-delivery systems, based on localized drug-delivery systems, have been developed to tackle the above-mentioned problems of particularly chemotherapy [2].

Polymeric nanofibers (NFs) have found much attention in medicine due to their high surface area-to-volume ratio, porosity, structural flexibility, and relatively easy fabrication [3]. They have been used for drug delivery [4, 5], cancer therapy and diagnosis [6], tissue engineering (e.g., wound dressing/healing) [7–11], photodynamic therapy [12], and bioelectronic devices [13]. For the purpose of drug delivery, numerous drug-loaded nanofibers have been designed using a variety of biopolymers [14] and biocompatible synthetic polymers such as poly(lactic acid) (PLA) [15], polycaprolactone (PCL) [16], polyvinyl alcohol (PVA) [17], and polyamide-6 (PA6) [18]. Each of the above-mentioned polymers has certain beneficial features and limitations. For instance, PCL possesses good durability but exhibits low mechanical strength and lacks cell binding sites [19]. Conversely, while PVA shows good flexibility, it suffers from low mechanical strength, limited biodegradability,

and its water solubility makes it unsuitable for wound dressing applications [19]. In contrast, polyamide-6 (i.e., nylon 6; polycaprolactam), as a synthetic, semicrystalline, biodegradable, and biocompatible polymer, offers excellent mechanical stability and high resistance to biological media [20]. Despite the high surface area of PA NFs, they exhibit a certain degree of brittleness, and the fabrication process involves the use of volatile solvents (e.g., formic acid, dimethylformamide) [21]. In general, PA proves to be a suitable base polymer for producing uniform and mechanically stable NFs.

Numerous techniques have been introduced to fabricate nanofibers such as template synthesis, bicomponent extrusion, self-assembly, phase separation, solution/melt blowing, centrifugal spinning, wet/dry/melt spinning, and electrospinning [3]. Among them, electrospinning (or electrohydrodynamic jetting) is an effective, accessible, variable, and straightforward technique, which is applicable to polymer solutions and melts [3, 22, 23]. Drug molecules can easily integrate into the polymer matrix before the electrospinning process and/or mix with the polymer during coaxial electrospinning [24]. It has been found that with the incorporation of the drug into the polymer, before electrospinning, the recrystallization of the drug is prevented [3]. One of the applications of electrospun nanofibers is to design implantable drug-loaded scaffolds [1] after the tumor resection (i.e., post-surgery treatment), and drug-loaded mats for wound dressing/healing [25]. In fact, the aim is drug delivery to the target (e.g., organ, tissue), release them at a sustained rate via a diffusion-controlled manner, and suppress the cytotoxicity of drugs [26].

Numerous electrospun nanofibrous mats have been developed for the localized delivery of drugs to the target such as poly(caprolactone)/poly(vinyl alcohol)/collagen loaded with *Momordica charantia* pulp extract for wound dressing [27], poly(vinyl alcohol)/gum tragacanth/MoS_2 electrospun for the delivery of tetracycline [28], and dextran/polycaprolactone/graphene oxide patch for transdermal delivery of antibiotic [29]. Moreover, PCL/soy protein isolate [30] and polyacrylonitrile/*Aloe Vera* extract [31]) were applied for wound healing, while ethyl cellulose/polyvinylpyrrolidone [32] was used in skin tissue engineering.

One of the primary challenges in the development of drug-delivery systems is mitigating the therapeutic impact of the drug due to a fast release profile. However, designing a sustained drug release system can ensure the drug's efficiency. To control release kinetics, a secondary carrier is generally employed to incorporate into the polymer matrix [6, 24]. For instance, cyclodextrin (CD) offers a well-defined cavity for hosting a variety of guest molecules particularly drugs. CDs are water-soluble and crystalline natural cyclic oligosaccharides, which are synthesized by cyclization of six to eight of D-glucopyranosyl residues via α-1,4-linkage [33]. There are three distinct types of CDs; α, β, and γ-CD, which are formed from six, seven, and eight building blocks, respectively. They have truncated cone-shaped structures with identical depths of ~0.8 nm and inner diameters of 0.57, 0.78, and 0.95 nm for α, β, and γ forms, respectively [34]. Among CDs, β-CD is an inexpensive form (due to the easier manner of purification) with a moderate cavity size [33]. The existence of hydroxyl groups on the secondary face (wider side) and hydroxymethyl groups on the primary face (narrow side) provide hydrophilic nature on the external part of the CDs [34], but β-CD has a low water solubility at room temperature. However,

the inner cavity shows less hydrophilicity (arising from glycosidic oxygens and C–H units) [35], which could be beneficial for a host–guest complex of organic molecules [36, 37]. CDs have been used not only in carrying drugs, but also in facilitating drug transport into the cells through membrane barriers [38]. It has been also found that CDs can preferably absorb in the colon rather than the stomach and small intestine [38], thus it can benefit the design of targeted drug-delivery systems.

In the current work, polyamide-based nanofibers were fabricated via an electrospinning technique for the delivery of the anticancer drug, doxorubicin (DOX). PA 6 was chosen as the base polymer due to its high biocompatibility, biodegradability, and mechanical stability [20]. β-CD was incorporated into the polymer matrix to control the release kinetics of the drug. Additionally, β-CD can stabilize DOX through the formation of a complex, inhibiting the self-association of DOX molecules. The pharmacological efficacy of the drug can be compromised by its tendency to aggregate [39]. The structure and physical properties of the as-prepared PA/β-CD/DOX patch were studied by SEM, TGA, FTIR, PXRD, and water contact angle. The swelling behaviors, drug loading/releasing, and cell viabilities were also evaluated.

Experimental

Chemicals

Polyamide (nylon 6; MW: 224.30 g mol^{-1}) was purchased from Poly-science, Inc. β-cyclodextrin, formic acid, methanol, and phosphate buffer saline (PBS) were purchased from Sigma–Aldrich. Doxorubicin hydrochloride (DOX: HCl, purity > 95%) was purchased from Iran Pharmaceutical Co. The LNCap was a human prostate cancer cell line purchased from LONZA Biologics (Slough, UK). Gentamicin (from Troge Medical, Germany), powder medium (from Gibco, UK), ethanol (99.9%, from Scharlau), and Trypsin-ethylenediaminetetraacetic acid (EDTA) powder (from Gibco, UK) were also obtained from suppliers.

Formation of β-CD/DOX complex

The β-CD/DOX complexes were prepared by mixing different molar ratios (1:1, 1:2, 1:3) of β-CD: DOX solutions. β-CD and DOX were initially dissolved separately in deionized water (30 mL) and then mixed by stirring for 12 h. The final solution was dehydrated by freeze-drying.

Fabrication of electrospun NFs

The NFs were prepared by dissolving polyamide (11.7% w/v) in formic acid and mixing with β-CD/DOX complex. The mixture was stirred for 12 h to form a homogeneous state. A semi-industrial electrospinning machine, made by Iran's Fanavaran Nanoscale Co., was used for electrospinning. The effective parameters of the electrospinning process were set accordingly by applying a spinning voltage of 25 kV and an advancement

rate of 0.5 mL h^{-1} at a receiving distance of 15 cm at room temperature. A grounded aluminum foil was used as a receiving device to collect nanofibers.

Characterization

The morphology of NFs was studied by scanning electron microscopy (SEM) using an XL30 Philips microscope with an accelerating voltage of 20.0 kV. The samples were sputtered with gold before analysis. The diameters of NFs were determined using Image-J and OriginLab software. Fourier transmission Infrared spectroscopy (FTIR) was used to investigate the presence of functional groups with a spectrophotometer of BIORAD-FTS-7PC. The thermal stability of the NFs was assessed by thermogravimetric analysis (Perkin Elmer, sta6000) at the heating rate of 10 °C min^{-1} under N_2 flow. Powder X-ray diffraction (PXRD) was used to record the crystalline structure of NFs using a Philips Pert Pro diffractometer with CuK*a* radiation ($\lambda = 1.54$ Å) at 40 kV. The contact angle technique (CA) was used to determine the degree of hydrophobicity or hydrophilicity of NFs surface. The measurement was carried out by a Drop Sessile method using an instrument (model: JIKAN) and the angles were determined using Image-J software. The drug loading and release were determined by a UV–vis spectrophotometer (Varian, Cary 100).

Water absorption test (Swelling test)

The capability of the NFs in the absorption of water was carried out at 37 °C (pH 7.4). A piece of NFs was weighed and then submerged in a water tank at different times of 15, 30, 90, 120, and 150 min. After that, the samples were withdrawn, dried with filter paper, and weighed again. The content of water absorption (W) is calculated using Eq. (1):

$$W = \left(W_1 - W_0\right)/W_0 \times 100 \tag{1}$$

The W_0 and W_1 are the weight of dry and wet NFs, respectively. An average value was obtained from three similar samples at the same conditions [40].

Encapsulation efficiency: drug loading and release

The encapsulation efficiency (EE %) was calculated by measuring the drug loading (DL %) of DOX in PA NFs using a UV–vis spectrophotometer at the λ_{max} of 286 nm (corresponding to DOX). The EE% and DL% are calculated using Eqs. (2) and (3), respectively:

$$EE\,(\%) = (X - Y)/X \times 100 \tag{2}$$

$$DL\,(\%) = (X/Z) \times 100 \tag{3}$$

where X is the primary concentration of DOX, Y is the concentration of remaining DOX in the solution, and Z is the weight of the freeze-dried NFs after DOX loading [41].

The drug release from NFs was investigated using a dialysis bag in phosphate buffer (pH = 5, 7.4, 9). Briefly, 100 mg of the sample was placed in a dialysis bag immersed in 50 mL phosphate buffer solution (pH = 7.4) and put on a shaker incubator (100 rpm at 25 ℃) for a different time interval. 2.0 mL of the solution was taken from the released medium at predetermined intervals, while a similar amount of buffer solution was replaced. The amount of DOX was determined using a spectrophotometer at the λ_{max} of 286 nm. The experiments were repeated identically three times.

Cell culture and treatment

Prostate cancer and LNCap cells were cultured in RPMI 1640 supplemented with 10% fetal bovine serum and gentamicin drug in a 5% humidified CO_2 atmosphere at 37 °C. The cells were detached using trypsin, washed twice with 5 mL PBS and centrifuged for 5 min at 1500 rpm. The cells were seeded in 96-well plates (5000 cells/well) and incubated at 37 °C for 24 h to adhere properly. After that, the cells were exposed to the PA NFs with different β-CD:DOX molar ratios (1:1, 1:2, 1:3). The exposure was carried out for three replicates. The treated 96-well plates were incubated at 37 °C for 24 h. Cell viability was determined using an MTT-based assay [42]. A microtiter plate reader measured the corresponding absorbance of the cells at the wavelength of 570 nm.

Results and discussion

Characterization of NFs

The electrospinning technique was used for the fabrication of polyamide (PA) NFs as a drug carrier of DOX. β-CD was employed to enhance the loading of the drug via an inclusion phenomenon. The as-prepared electrospun NFs were thoroughly characterized by SEM, FTIR, PXRD, and swelling tests. Figure 1 shows the SEM images of NFs with different loading of β-CD/DOX complex. The NFs were uniform with good smoothness on the surface without the formation of any beads or defects. The addition of additives, DOX and/or β-CD/DOX, into the polymer matrix, did not generate any defect or inhomogeneity in the structure of the NFs. The diameter of the NFs was measured, and the results of size dispersity are given in Fig. 1. The diameter of NFs can be controlled by several parameters such as material composition, drawing speed, and solvent evaporation rate [12]. Since the latter two parameters remained almost constant during the fabrication, the composition of the polymer solution becomes the primary determining factor. It was found that by the addition of DOX into PA, the average diameter of the resulting NFs decreased from 139 ± 38 nm to 122 ± 32 nm. It might be due to the reduction of PA viscosity

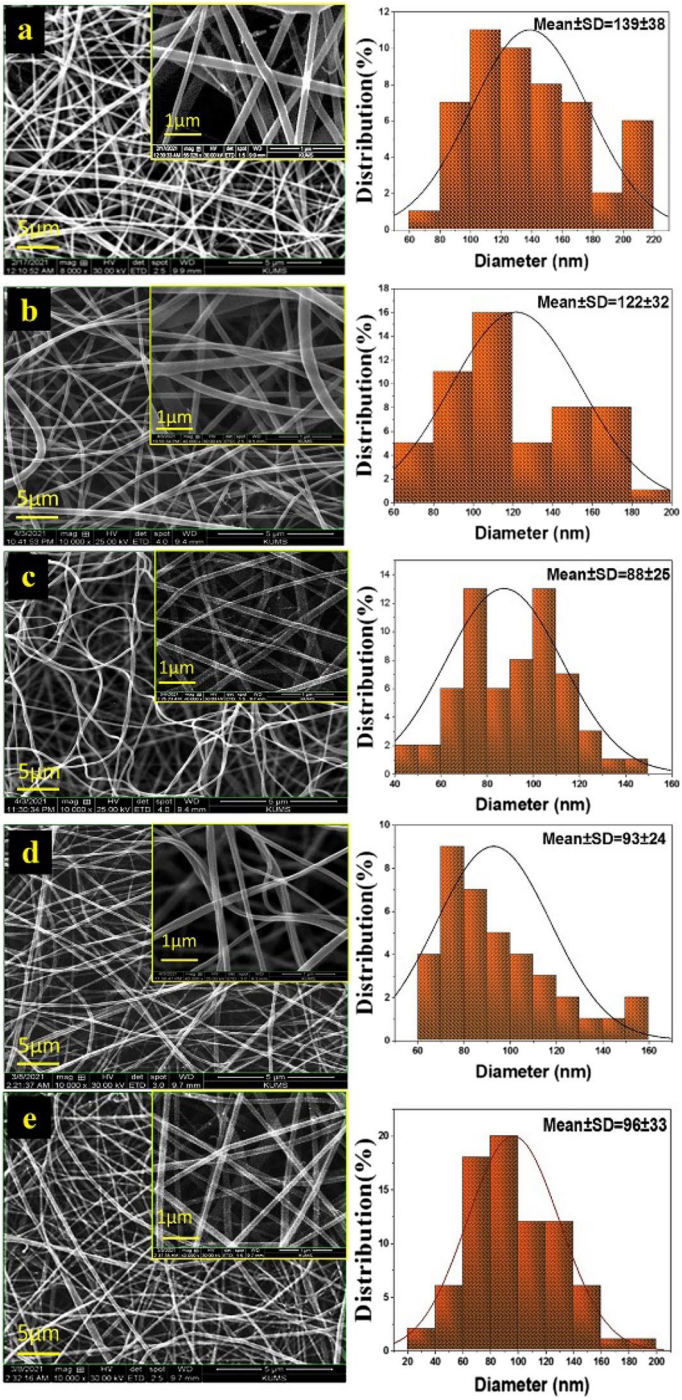

Fig. 1 SEM images of **a** PA, **b** PA/DOX, **c** PA/β-CD/DOX (1:1), **d** PA/β-CD/DOX (1:2), **e** PA/β-CD/DOX (1:3)

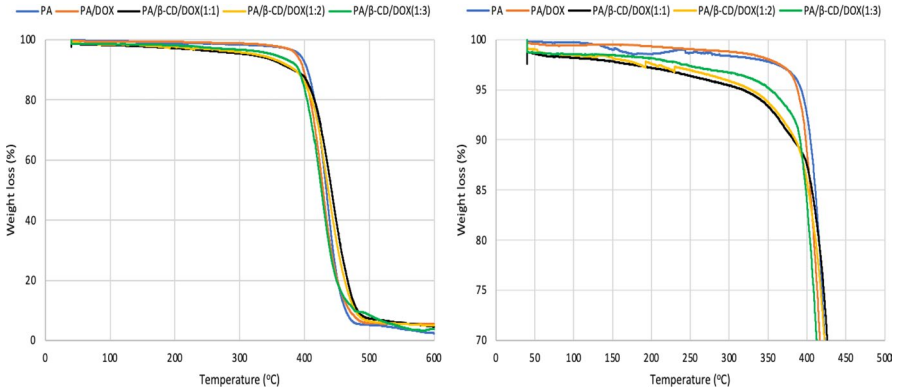

Fig. 2 The TGA curves of PA, β-CD, PA/DOX, and PA/β-CD/DOX (1:1, 1:2, 1:3) NFs

caused by the incorporation of DOX. Monteiro et al. reported [43] that conductivity and viscosity of the polymer solution can influence NFs diameters. They found that the introduction of tetracycline and tetracycline/β-CD (1:1 ratio) in a certain amount resulted in a reduction in the diameter of PCL due to a decrease in the conductivity and viscosity of the precursor mixture solution. Further reduction in the size was also observed for the NFs with the incorporation of β-CD/DOX complex. Although the addition a higher amount of DOX had no adverse effect on the morphology of the NFs, the corresponding diameter increased (Fig. 1d, e). The increase in diameter might be attributed to the increased viscosity of the polymer solution with the further addition of the drug [4, 9]. A similar result was reported by Ranjbar-Mohammadi and Bahrami, where the diameter of PCL increased with the rising viscosity of the polymer solution containing gum tragacanth [44]. The smoothness in the morphology of NFs indicates that the drug complex (i.e., β-CD/DOX) was uniformly distributed in the polymer matrix.

The thermal stability of NFs was investigated by thermogravimetric analysis (TGA). The TGA curves (Fig. 2) showed that PA NFs were stable up to 400 °C. By incorporation of the DOX and β-CD/DOX complex into the PA, the thermal stability of the resulting PA/β-CD/DOX NFs was reduced and the structures started to degrade at the temperature above 350 °C. This temperature is correlated to the degradation of β-CD as the thermal behavior of β-CD showed two obvious regimes corresponding to the dehydration and degradation above 100 (14 wt.% mass loss) and 300 °C (86 wt.% mass loss), respectively [43, 45]. By inclusion DOX to β-CD, the thermal stability of PA/β-CD did not change.

Figure 3 exhibits the FTIR spectra of the NFs, β-CD, and DOX. The spectrum of PA NFs showed the vibration bands at 3305, 2931, 2860, 1645, and 1539 cm^{-1} corresponding to the stretching N–H, asymmetric C–H, symmetric C–H, C=O, and bending N–H bonds, respectively [46]. In the spectrum of β-CD, the characteristic vibration modes were found at 3363 (O–H), 2926 (stretching C–H), 1641 cm^{-1} (bending O–H), and 1029 (C–O–C) cm^{-1} [47]. For DOX, the absorption bands of 3430, 1635, and 1093 cm^{-1} were assigned to the stretching O–H, bending N–H, and

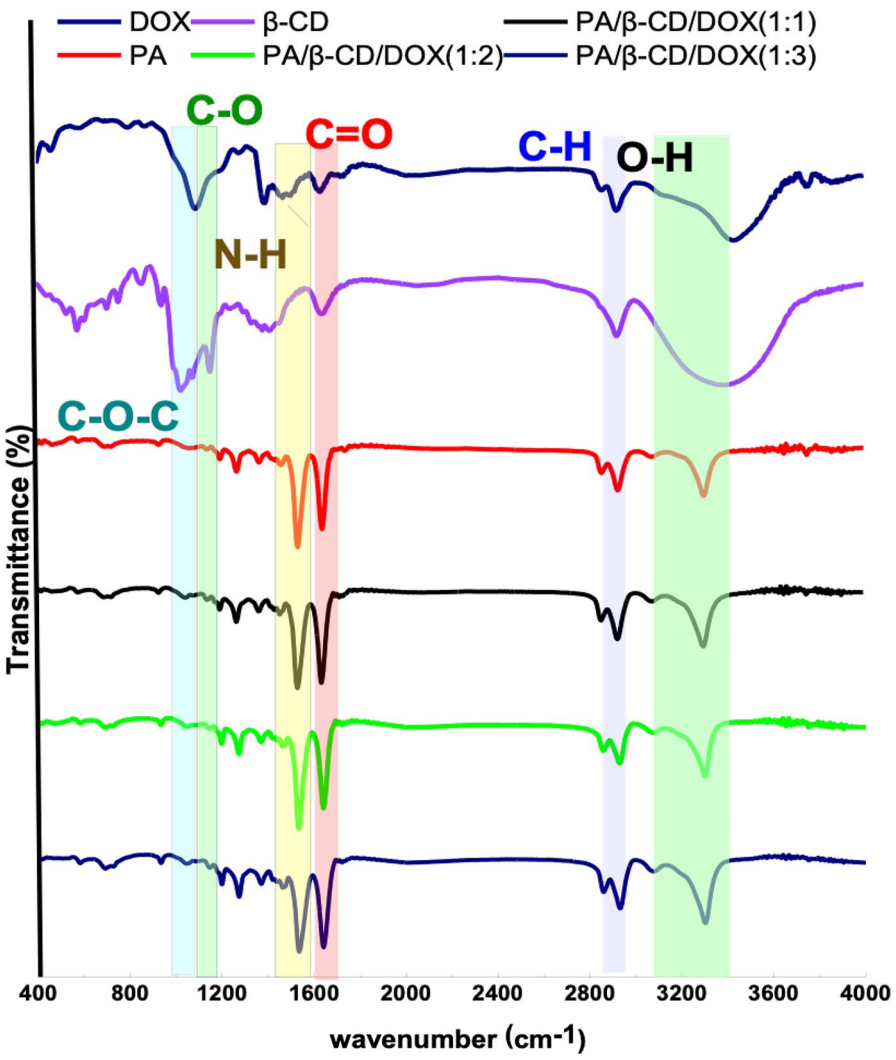

Fig. 3 FTIR spectra of PA, β-CD, DOX, and PA/β-CD/DOX (1:1, 1:2, 1:3)

stretching C–O vibrations, respectively [45]. The spectrum of PA/β-CD/DOX show a combination of the characteristic peaks of the components. Two new peaks at 1273 and 1197 cm^{-1} were probably related to a peak overlapping of DOX and β-CD with those in PA peaks.

The PXRD patterns (Fig. 4) for NFs demonstrated two signals at 2θ of 21° and 23.8°, which were identical to the characteristic peaks of PA [46]. The broad peaks observed in PA can be associated to the formation of crystalline defects during the electrospinning process [46]. By the addition of DOX and β-CD/DOX into PA, the corresponding broad peak of PA significantly intensified and split into two peaks,

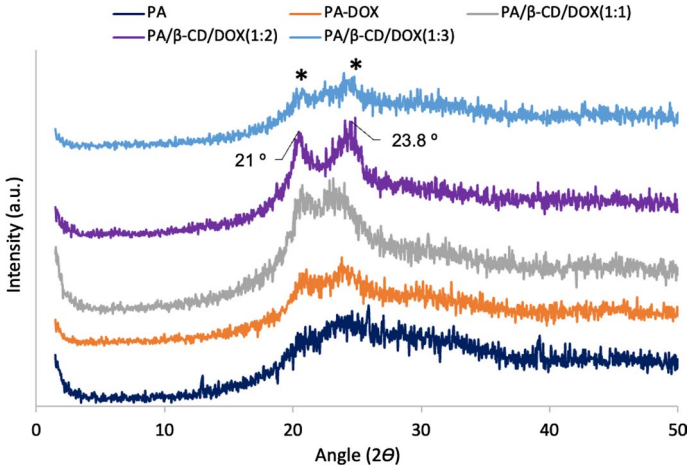

Fig. 4 PXRD patterns of PA, PA/DOX, and PA/β-CD/DOX (1:1, 1:2, 1:3)

indicating a higher degree of crystallinity in PA/β-CD/DOX. It appears that the crystallinity of β-CD and DOX contributes to the enhanced crystallinity of PA/β-CD/DOX. Conversely, the crystallinity of the β-CD/DOX complex and its structural order may decrease with an increase in the number of DOX molecules in the complex in PA/β-CD/DOX(1:3). It can be inferred a higher structural order and a greater stability constant in a complex formed between β-CD and monomeric or dimeric DOX [48].

The water contact angle measurement was conducted to determine the degree of hydrophilicity/hydrophobicity of NFs (Fig. 5). PA exhibited a hydrophilic nature, with a contact angle of ~ 55.9 ± 4°, due to the presence of amide groups. The contact angle of PA was increased to ~ 59.2 ± 4° after the introduction of β-CD, indicating a reduction in hydrophilicity. In addition, the contact angle was further increased with the addition of DOX and β-CD/DOX into PA. The corresponding values of 60.7°, 61.9°, 60.0°, and 65.9° were obtained for PA/DOX, PA/β-CD/DOX(1:1), PA/β-CD/DOX(1:2), and PA/β-CD/DOX(1:3), respectively. By increasing the hydrophobicity of PA/β-CD/DOX compared to PA, the compatibility of the drug carrier with the body's internal membrane, which is hydrophobic nature, is enhanced, thereby facilitating drug release.

Swelling test

The swelling test is typically used to evaluate the ability of polymeric materials to absorb solvent in their polymeric networks, and the nature and amount of interaction between polymer and solvent. PA exhibits hydrophilicity through the hydrogen bonding of amide groups with water, while the addition of β-CD reduces the hydrophilicity (water resistance), therefore the swelling behavior can be tuned with additives. Figure 6 displays the degree of swelling (inflation rate) of different NFs in water. As can be expected, with the addition of β-CD/DOX complex into the PA

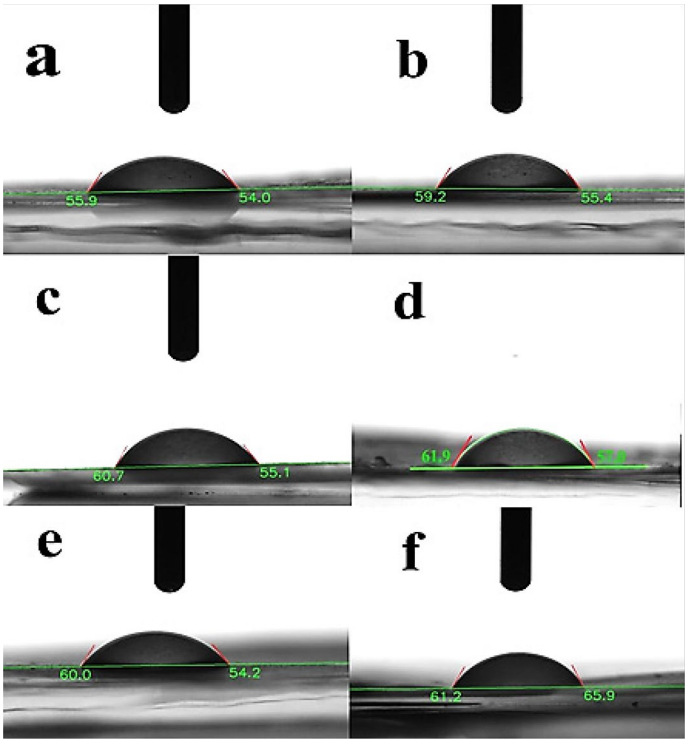

Fig. 5 Water contact angle of **a** PA, **b** PA/β-CD, **c** PA/DOX, **d** PA/β-CD/DOX (1:1), **e** PA/β-CD/DOX (1:2), and **f** PA/β-CD/DOX (1:3)

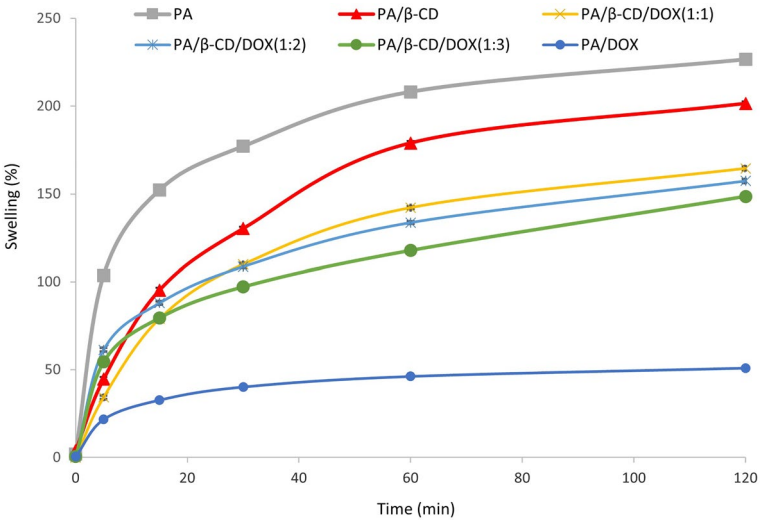

Fig. 6 Swelling test for PA, PA/β-CD, PA/DOX, and PA/β-CD/DOX (1:1,1:2,1:3)

Table 1 Encapsulation efficiency and drug loading of nanofibers

NFs	EE (%)	DL (%)
PA/DOX	97.4 ± 4.6	47.2 ± 1.0
PA/β-CD/DOX(1:1)	98.6 ± 2.4	55.1 ± 2.6
PA/β-CD/DOX(1:2)	91.6 ± 7.0	55.9 ± 2.9
PA/β-CD/DOX(1:3)	89.8 ± 5.6	53.1 ± 1.6

NFs the swelling degree was reduced, and a further increase in β-CD/DOX ratio caused more reduction in the water absorption. Therefore, the composite NFs can be sufficiently stable in the presence of water, which could be beneficial for real applications in biological systems.

Encapsulation efficiency and drug release

By immersing PA in a solution of β-CD/DOX with different β-CD:DOX ratios of 1:1, 1:2, 1:3, the EE and DL were calculated for the nanofibers (Table 1). The drug loading in PA/DOX was attributed to the encapsulation of the drug molecules within the polymeric network of the NFs. The presence of β-CD further enhanced drug loading through strong interactions between β-CD and DOX.

The capability of the drug-loaded PA in the release of the drug was investigated in different pH (5, 7.4, 9) for four days (Fig. 7). Given the pH difference between healthy (pH = 7.4) and abnormal (pH = 4–6) tissues, an acidic medium (pH = 5) was examined to simulate conditions on the surface of cancer cells [49]. Additionally, pH = 9 was selected to study due to the weak alkaline conditions associated with chronic wounds [50, 51]. The fastest rate of drug release was observed in the first 10 h for all drug carriers. PA/DOX exhibited the highest drug release of ~ 55% within 10 h and the release continued slowly over time to reach a maximum release of ~ 77%. For PA/β-CD/DOX samples, a drug release of ~ 33–38% was observed in 10 h and the release continuously increased to a maximum of ~ 90–93%. Among PA/β-CD/DOX NFs, PA/β-CD/DOX(1:1) showed higher total release (~ 93%) than PA/β-CD/DOX(1:2) and PA/β-CD/DOX(1:3). The results indicated that β-CD can control the release of DOX by slowing down the rate of release. The slowest drug release rate was found for PA/β-CD/DOX(1:3). The effect of pH on the release behavior was not significant for all samples, however, the pH of 7.4, real physiological conditions, showed a higher rate of release. The acidic medium (pH = 5) demonstrated a drug release profile comparable to that of other conditions. Consequently, the results demonstrate that PA/β-CD/DOX prevents the premature release of drugs at undesirable sites while enabling controlled release at target sites.

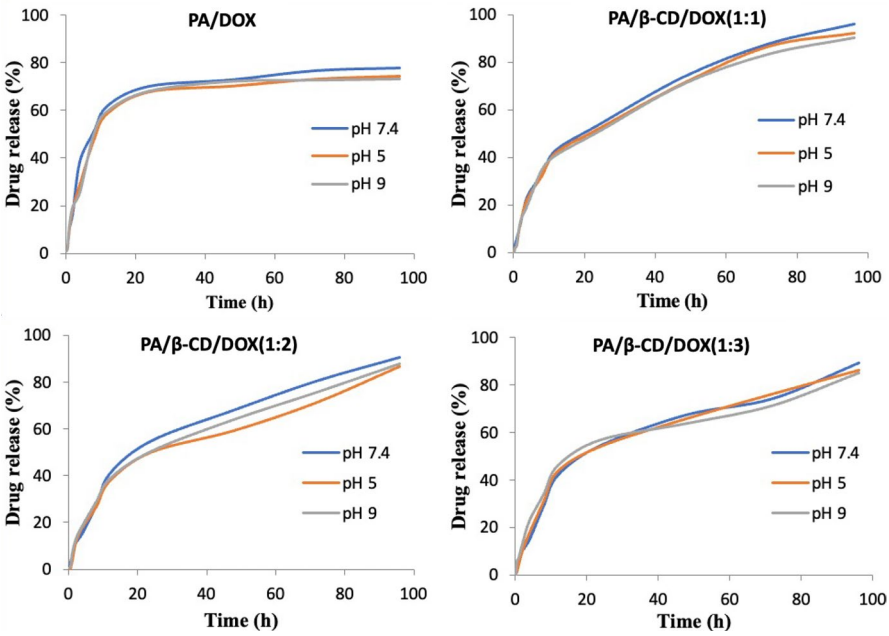

Fig. 7 Drug release profiles for PA/DOX, PA/β-CD/DOX (1:1), PA/β-CD/DOX (1:2), and PA/β-CD/DOX (1:3) in pH = 5, 7.4, and 9

Cell culture and treatment

Prostate cancer and LNCap cells were cultured for in vitro treatment with DOX-loaded NFs. Figure 8 illustrates cell viability (or cell proliferation) in the presence of PA, β-CD, DOX, and PA/β-CD/DOX(1:1,1:2,1:3) in three replicates (H, M, and L) according to the reported protocol [42]. PA showed the lowest inhibition rate of cell growth (3.5–14.2%), while free DOX demonstrated the highest inhibition (17.1–50.9%) among the samples. Notably, free β-CD solution exhibited a relatively high inhibition percentage (37.0–38.7%). These findings indicate that pure PA NFs have low cellular toxicity. However, a significant level of toxicity is evident in the case of free β-CD. The incorporation of β-CD/DOX into PA and the controlled release of the drug resulted in moderate and mild inhibition rates of 10.7–28.7%, 15.9–28.2%, and 14.3–18.8% for PA/β-CD/DOX(1:1), PA/β-CD/DOX(1:2), and PA/β-CD/DOX(1:3), respectively. In other words, the higher cell viability observed under PA/β-CD/DOX(1:1,1:2,1:3) exposure, compared to free DOX, can be attributed to the slower drug release from drug-loaded NFs. Therefore, PA/β-CD/DOX NFs hold promise as drug carriers for sustained and controlled release systems.

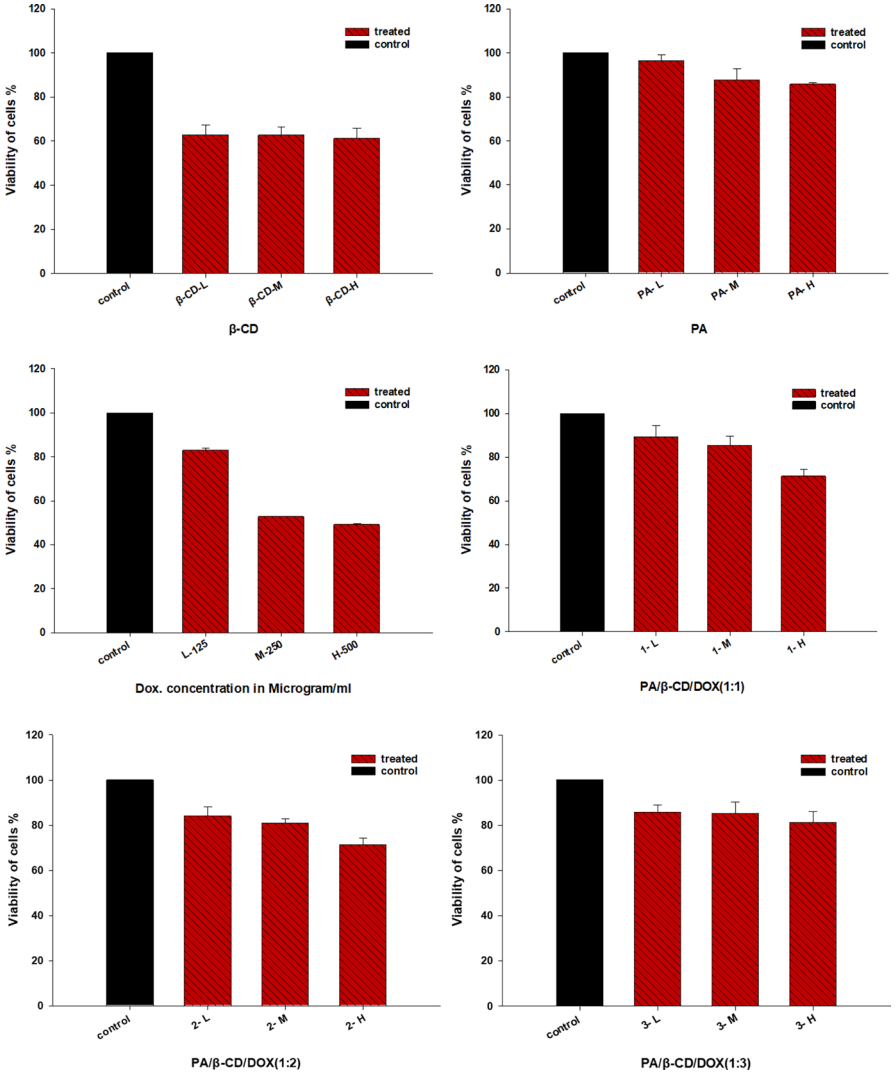

Fig. 8 The cell growth measurement in the presence of NFs after 24 h incubation. The viability of control cells was set at 100%

Conclusion

In the present study, PA-based nanocarriers were designed for the controlled release of anticancer drug DOX. To enhance the loading of DOX, β-CD with available cavity inside the structure was used for encapsulation of DOX. The defect-free PA NFs containing the incorporated β-CD/DOX complex were prepared via electrospinning. The resulting NFs had diameters ranging from 88 to 96 nm, which were smaller than those of pure PA (139 nm) and PA/DOX (122 nm). The presence of the β-CD/

DOX complex in the PA NFs led to a reduction in hydrophilicity, as evidenced by an increase in the contact angle altered from ~56° to >60°, and a decrease in the swelling capacity of the drug-loaded NFs. The incorporation of β-CD into the PA NFs resulted in an increased DOX loading of 56% in PA/β-CD/DOX, compared to 47% in PA/DOX. Moreover, the NFs exhibited a slower drug release over a period of at least four days and a total drug release ranging from 90 to 93%. In contrast, NFs without β-CD showed a faster drug release during the same time frame, with a total drug release of 77%. The lower cell viability observed in DOX-loaded NFs against LNCap cancer cells can be attributed to the slower release of drug. Consequently, electrospun NFs emerge as a suitable platform for the loading and delivery of drugs under controlled manner. We anticipate that PA/β-CD/DOX NFs will gain high attention in the advancement of effective drug delivery and release systems for chemotherapeutic medicines.

Acknowledgements Authors acknowledge Razi University, Kermanshah University of Medical Sciences, Babylon University (Iraq) for the partial financial support.

Declarations

Conflict of interest The authors declare that they have no known competing financial interests or personal relationships that could have appeared to influence the work reported in this paper.

References

1. Li D, Chen Y, Zhang Z, Chen M (2018) Mesoporous nanofibers mediated targeted anti-cancer drug delivery. MRS Adv 425:2991–3002
2. Aberoumandi SM, Mohammadhosseini M, Abasi E, Saghati S, Nikzamir N, Akbarzadeh A, Panahi Y, Davaran S (2017) An update on applications of nanostructured drug delivery systems in cancer therapy: a review. Nanomed Biotechnol 45:1058–1068
3. Deshmukh S, Kathiresan M, Kulandainathan MA (2022) A review on biopolymer-derived electrospun nanofibers for biomedical and antiviral applications. Biomater Sci 10:4424–4442
4. Balaji A, Vellayappan MV, John AA, Subramanian AP, Jaganathan SK, Supriyanto E, Razak SIA (2015) An insight on electrospun-nanofibers-inspired modern drug delivery system in the treatment of deadly cancers. RSC Adv 5:57984–58004
5. Hussain T, Ramakrishna S, Abid S (2022) Nanofibrous drug delivery systems for breast cancer: a review. Nanotechnology 33:102001
6. Ding Y, Li W, Zhang F, Liu Z, Zanjanizadeh Ezazi N, Liu D, Santos HA (2019) Electrospun fibrous architectures for drug delivery, tissue, engineering and cancer therapy. Adv Funct Mater 29:1802852
7. John JV, McCarthy A, Karan A, Xie J (2022) Electrospun nanofibers for wound management. ChemNanoMat 8:e202100349
8. Gao Y, Qiu Z, Liu L, Li M, Xu B, Yu D, Qi D, Wu J (2022) Multifunctional fibrous wound dressings for refractory wound healing. J Polym Sci 60:2191–2212
9. Gao C, Zhang L, Wang J, Jin M, Tang Q, Chen Z, Cheng Y, Yang R, Zhao G (2021) Electrospun nanofibers promote wound healing: theories, techniques, and perspectives. J Mater Chem B 9:3106–3130
10. Afsharian YP, Rahimnejad M (2021) Bioactive electrospun scaffolds for wound healing applications: a comprehensive review. Polym Testing 93:106952
11. Zhang X, Li L, Ouyang J, Zhang L, Xue J, Zhang H, Tao W (2021) Electroactive electrospun nanofibers for tissue engineering. Nano Today 39:101196

12. Nadaf A, Gupta A, Hasan N, Fauziya AS, Kesharwani P, Ahmad FJ (2022) Recent update on electrospinning and electrospun nanofibers: current trends and their applications. RSC Adv 12:23808–23828
13. Majumder S, Sagor MMH, Arafat MT (2022) Functional electrospun polymeric materials for bioelectronic devices: a review. Mater Adv 3:6753–6772
14. Kumar A, Sinha-Ray S (2018) A review on biopolymer-based fibers via electrospinning and solution blowing and their applications. Fibers 6:45
15. Liu J, Shi R, Hua Y, Gao J, Chen Q, Xu L (2021) A new cyanoacrylate-poly(lactic acid)-based system for a wound dressing with on-demand removal. Mater Lett 293:129666
16. Mitxelena-Iribarren O, Riera-Pons M, Pereira S, Calero-Castro FJ, Tuñón JMC, Padillo-Ruiz J, Mujika M, Arana S (2023) Drug-loaded PCL electrospun nanofibers as anti-pancreatic cancer drug delivery systems. Polym Bull 80:7763–7778
17. Yan E, Jiang J, Yang X, Fan L, Wang Y, An Q, Zhang Z, Lu B, Wang D, Zhang D (2020) pH-sensitive core-shell electrospun nanofibers based on polyvinyl alcohol/polycaprolactone as a potential drug delivery system for the chemotherapy against cervical cancer. J Drug Deliv Sci Technol 55:101455
18. Nirmala R, Navamathavan R, Park SJ, Kim HY (2014) Recent progress on the fabrication of ultrafine polyamide-6 based nanofibers via electrospinning: a topical review. Nano-Micro Lett 6:89–107
19. Zhang X, Wang Y, Gao Z, Mao X, Cheng J, Huang L, Tang J (2024) Advances in wound dressing based on electrospinning nanofibers. J Appl Polym Sci 141:e54746
20. Darwish MSA, Bakry A, Kolek O, Martinová L, Stibor I (2019) Electrospun functionalized magnetic polyamide 6 composite nanofiber: fabrication and stabilization. Polym Compos 40:296–303
21. Abdul Hameed MM, Khan SAPM, Thamer BM, Rajkumar N, El-Hamshary H, El-Newehy M (2023) Electrospun nanofibers for drug delivery applications: methods and mechanism. Polym Adv Technol 34:6–23
22. Snetkov P, Morozkina S, Olekhnovich R, Uspenskaya M (2022) Electrospun curcumin-loaded polymer nanofibers: solution recipes, process parameters, properties, and biological activities. Mater Adv 3:4402–4420
23. Yazawa K, Mizukami S, Aoki M, Tamada Y (2022) Electrospinning of spider silk-based nanofibers. Polym Adv Technol 33:2637–2644
24. Contreras-Cáceres R, Cabeza L, Perazzoli G, Díaz A, López-Romero JM, Melguizo C, Prados J (2019) Electrospun nanofibers: recent applications in drug delivery and cancer therapy. Nanomaterials 9:656
25. Khan AR, Morsi Y, Zhu T, Ahmad A, Xie X, Yu F, Mo X (2021) Electrospinning: an emerging technology to construct polymer-based nanofibrous scaffolds for diabetic wound healing. Front Mater Sci 15:10–35
26. Khodadadi M, Alijani S, Montazeri M, Esmaeilizadeh N, Sadeghi-Soureh S, Pilehvar-Soltanahmadi Y (2020) Recent advances in electrospun nanofiber-mediated drug delivery strategies for localized cancer chemotherapy. J Biomed Mater Res 108:1444–1458
27. Salami MS, Bahrami G, Arkan E, Izadi Z, Miraghaee S, Samadian H (2021) Co-electrospun nanofibrous mats loaded with bitter gourd (Momordica charantia) extract as the wound dressing materials: in vitro and in vivo study. BMC Complem Med Therap 21:111
28. Khaledian S, Kahrizi D, Balaky STJ, Arkan E, Abdoli M, Martinez F (2021) Electrospun nanofiber patch based on gum tragacanth/polyvinyl alcohol/molybdenum disulfide composite for tetracycline delivery and their inhibitory effect on Gram+ and Gram− bacteria. J Mol Liquids 334:115989
29. Nematpour N, Farhadian N, Ebrahimi KS, Arkan E, Seyedi F, Khaledian S, Shahlaei M, Moradi S (2020) Sustained release nanofibrous composite patch for transdermal antibiotic delivery. Colloids Surf A 586:124267
30. Doustdar F, Ramezani S, Ghorbani M, Mortazavi Moghadam F (2022) Optimization and characterization of a novel tea tree oil-integrated poly (ε-caprolactone)/soy protein isolate electrospun mat as a wound care system. Int J Pharma 627:122218
31. Alvandi H, Jaymand M, Eskandari M, Aghaz F, Hosseinzadeh L, Heydari M, Arkan E (2023) A sandwich electrospun nanofibers/Tragacanth hydrogel composite containing Aloe vera extract and silver sulfadiazine as a wound dressing. Polym Bull 80:11235–11248
32. Doustdar F, Ghorbani M (2022) ZIF-8 enriched electrospun ethyl cellulose/polyvinylpyrrolidone scaffolds: the key role of polyvinylpyrrolidone molecular weight. Carbohydr Polym 291:119620

33. Wang S, Shao G, Zhao H, Yang L, Zhu L, Liu H, Cui B, Zhu D, Li J, He Y (2021) Covering soy polysaccharides gel on the surface of β-cyclodextrin-based metal–organic frameworks. J Mater Sci 56:3049–3061
34. Roy I, Stoddart JF (2021) Cyclodextrin metal−organic frameworks and their applications. Acc Chem Res 54:1440–1453
35. Rajkumar T, Kukkar D, Kim KH, Sohn JR, Deep A (2019) Cyclodextrin-metal–organic framework (CD-MOF): from synthesis to applications. J Ind Eng Chem 72:50–66
36. Moussa Z, Hmadeh M, Abiad MG, Dib OH, Patra D (2016) Encapsulation of curcumin in cyclodextrin-metal organic frameworks: Dissociation of loaded CD-MOFs enhances stability of curcumin. Food Chem 212:485–494
37. Sha JQ, Zhong XH, Wu LH, Liu GD, Sheng N (2016) Nontoxic and renewable metal–organic framework based on α-cyclodextrin with efficient drug delivery. RSC Adv 6:82977–82983
38. Liu Z, Ye L, Xi J, Wang J, Feng ZG (2021) Cyclodextrin polymers: Structure, synthesis, and use as drug carriers. Prog Polym Sci 118:101408
39. Anand R, Malanga M, Manet I, Manoli F, Tuza K, Aykaç A, Ladavière C, Fenyvesi E, Vargas-Berenguel A, Gref R, Monti S (2013) Citric acid–γ-cyclodextrin crosslinked oligomers as carriers for doxorubicin delivery. Photochem Photobiol Sci 12:1841–1854
40. Sahoo S, Sasmal A, Sahoo D, Nayak P (2010) Synthesis and characterization of chitosan-polycaprolactone blended with organoclay for control release of doxycycline. J Appl Polym Sci 118:3167–3175
41. Doostan M, Maleki H, Doostan M, Khoshnevisan K, Faridi-Majidi R, Arkan E (2021) Effective antibacterial electrospun cellulose acetate nanofibrous patches containing chitosan/erythromycin nanoparticles. Int J Biolog Macromol 168:464–473
42. Kamiloglu S, Sari G, Ozdal T, Capanoglu E (2020) Guidelines for cell viability assays. Food Front 1:332–349
43. Monteiro APF, Rocha CMSL, Oliveira MF, Gontijo SML, Agudelo RR, Sinisterra RD, Cortés ME (2017) Nanofibers containing tetracycline/β-cyclodextrin: physico-chemical characterization and antimicrobial evaluation. Carbohydr Polym 156:417–426
44. Ranjbar-Mohammadi M, Bahrami SH (2016) Electrospun curcumin loaded poly(ε-caprolactone)/gum tragacanth nanofibers for biomedical application. Int J Biolog Macromol 84:448–456
45. Neacșu A (2018) Physicochemical investigation of the complexation between γ-cyclodextrin and doxorubicin in solution and in solid state. Thermochim Acta 661:51–58
46. Yang W, Li R, Fang C, Hao W (2019) Surface modification of polyamide nanofiber membranes by polyurethane to simultaneously improve their mechanical strength and hydrophobicity for breathable and waterproof applications. Prog Org Coat 131:67–72
47. Volkova T, Surov A, Terekhova I (2020) Metal–organic frameworks based on β-cyclodextrin: design and selective entrapment of non-steroidal anti-inflammatory drugs. J Mater Sci 55:13193–13205
48. Anand R, Ottani S, Manoli F, Manet I, Monti S (2012) A close-up on doxorubicin binding to c-cyclodextrin: an elucidating spectroscopic, photophysical and conformational study. RSC Adv 2:2346–2357
49. Li M, Luo Z, Zhao Y (2016) Hybrid nanoparticles as drug carriers for controlled chemotherapy of cancer. Chem Rec 16:1833–1851
50. Kassal P, Zubak M, Scheipl G, Mohr GJ, Steinberg MD, Steinberg IM (2017) Smart bandage with wireless connectivity for optical monitoring of pH. Sens Actuators B 246:455–460
51. Alves PM, Barrias CC, Gomes P, Martins MCL (2021) Smart biomaterial-based systems for intrinsic stimuli-responsive chronic wound management. Mater Today Chem 22:100623